C. C. Poe, Jr.[1]

Fatigue Crack Propagation in Stiffened Panels

REFERENCE: Poe, C. C., Jr., **"Fatigue Crack Propagation in Stiffened Panels,"** *Damage Tolerance in Aircraft Structures, ASTM STP 486*, American Society for Testing and Materials, 1971, pp. 79–97.

ABSTRACT: Rates of fatigue crack growth were measured in fatigue tests of stiffened panels constructed with bolted and integral stringers. The panels with bolted stringers were made from 2024-T3 aluminum alloy sheet with either aluminum alloy or steel stringers. The stringers were attached to the sheet with interference fit lock bolts. Stringer spacing and stiffness were varied systematically in the construction of the panels. The integrally stiffened panels were made from 7075-T6 aluminum alloy sheet extruded with outstanding stringers.

The stress intensity factor, calculated by a previously developed method, is used to predict the crack growth rates for the stiffened panels. Fatigue tests were conducted on unstiffened panels to determine the relationship between the stress intensity factor and crack growth rate.

In general, the stress intensity factor correctly predicts the crack growth rates in panels with bolted and with integral stringers except when the cracks are long. In these cases, the measured rates are slightly higher than the predicted rates. Furthermore, the stress intensity factor correctly predicts the rates to be lower in the panels with stiffer and more closely spaced stringers and to be equal in panels with steel and with aluminum alloy stringers of equal stiffness. The bolted stringers reduced the crack growth rate significantly below that for an equally stressed unstiffened panel, whereas the integral stringers had no significant effect.

KEY WORDS: aircraft, aircraft panels, joists, stiffening, fatigue (materials), cracking (fracturing), crack propagation, cyclic loads, axial stress, stress cycles, tensile properties, inspection, fatigue tests, aluminum alloys, structural steels

Nomenclature

- a Half length of crack in sheet, measured from panel center line, in. (mm)
- a_{st} Length of crack in integral stringer, in. (mm)
- A Gross cross-sectional area of sheet, in.^{2} (m^2)
- A_{st} Total gross cross-sectional area of stringers, in.^{2} (m^2)
- b Spacing of stringers, in. (mm)
- C Empirical constant

[1] Aerospace technologist, Fatigue Branch, Langley Research Center, National Aeronautics and Space Administration, Langley Station, Hampton, Va. 23365.

E Young's modulus of elasticity for sheet material, ksi (MN/m^2)
E_{st} Young's modulus of elasticity for stringer material, ksi (MN/m^2)
F Cumulative distribution function
K Stress intensity factor, ksi$\sqrt{in.}$ ($MN/m^{3/2}$)
K_c Critical value of stress intensity factor, ksi$\sqrt{in.}$ ($MN/m^{3/2}$)
K_{max} Stress intensity factor corresponding to maximum value of cyclic load, ksi$\sqrt{in.}$ ($MN/m^{3/2}$)
ΔK Range of the stress intensity factor, K_{max} $(1 - R)$, ksi$\sqrt{in.}$ ($MN/m^{3/2}$)
n Empirical constant
N Number of cycles of load
p Spacing of rivets, in. (mm)
r, θ Plane polar coordinates, in. (mm), deg
R Ratio of minimum to maximum values of cyclic load
S Gross stress in sheet, ksi (MN/m^2)
S_{max} Maximum cyclic gross stress in sheet, ksi (MN/m^2)
t_{st} Thickness of stringer material, in. (mm)
w Width of stringers, in. (mm)
W Width of unstiffened panel, in. (mm)
x, y Cartesian coordinates, in. (mm)
$(da/dN)_m$ Rate of growth of fatigue crack measured in panels without stringers, in./cycle (mm/cycle)
ϵ Exponential of error in method of least squares
μ Ratio of stringer stiffness to total stiffness
$\sigma_{xx}, \sigma_{xy}, \sigma_{zz}$ Normal stress components, ksi (MN/m^2)
$\tau_{xy}, \tau_{xz}, \tau_{yz}$ Shearing stress components, ksi (MN/m^2)

Long fatigue life and minimum structural weight are conflicting design requirements for aircraft structures. Because of the importance of low structural weight, allowable stresses cannot be lowered to eliminate totally the occurrence of fatigue cracks. For this reason, the structural integrity of a large portion of the commercial and military aircraft fleet today depends on some type of inspection procedure to detect fatigue cracks before they attain a critical length and cause catastrophic failure. If efficient and reliable inspection intervals are to be established, accurate analytical methods for predicting the rate of growth of a fatigue crack in an aircraft structure must be developed.

Numerous investigations have demonstrated that in a particular material the rate of fatigue crack growth for constant amplitude loading is related uniquely to the stress intensity factor (K-rate relationship). Figge and Newman [*1*][2] have demonstrated that stress intensity factor calculations and the K-rate relationship determined from tests of simple specimens can be used to predict fatigue crack growth rates in specimens subjected to various combinations of uniformly distributed and concentrated forces.

[2] Italic numbers in brackets refer to the list of references at the end of this paper.

The stiffened panel is representative of a large portion of aircraft construction and therefore has much practical importance. The stress intensity factor for a stiffened panel containing a crack in the sheet material and having riveted stringers of uniform size and spacing has been calculated and is presented in Ref *2*. Stringer stiffness, stringer spacing, and rivet spacing were parameters in those calculations. The purpose of the present investigation is to demonstrate that the stress intensity factor calculated by the method in Ref *2* can be used to predict the rate of growth of a fatigue crack in a stiffened panel; thus, a comparison is made of measured and predicted crack growth rates in stiffened panels subjected to constant amplitude fatigue loading.

The specimens were constructed of 2024-T3 aluminum alloy sheet with bolted stringers of aluminum alloy or steel and of 7075-T6 aluminum alloy sheet extruded with integral stringers. The bolted stringers were attached with interference fit lock bolts. Stringer stiffness and stringer spacing were varied in the construction of the panels with bolted stringers. The K-rate relationships were determined from crack growth rates measured in unstiffened panels made from the same 2024-T3 and 7075-T6 materials. The method in Ref *2* also is extended to calculate the stress intensity factor for the panels with integral stringers.

Specimens

Panels with Bolted Stringers

Six stiffened panels were made with bolted stringers of various spacing, stiffness, and material as shown in Table 1. The stiffness of the stringers is given in terms of a dimensionless parameter μ where

$$\mu = \frac{A_{st}E_{st}}{AE + A_{st}E_{st}} \quad \ldots\ldots\ldots\ldots\ldots\ldots\ldots\ldots\ldots\ldots (1)$$

which is the ratio of stringer stiffness to total panel stiffness. The panel material was 0.090-in. (2.29-mm)-thick 2024-T3 aluminum alloy sheet. The stringer materials were 2024-T3 and 2024-T4 aluminum alloys and AM350-CRT steel. The two panels with steel stringers were made with the stringer stiffness and spacing identical to two of the panels with aluminum alloy stringers. Figure 1 shows the basic configuration of the panels. The stringers were attached to the sheet material by ¼-in. (6.4-mm) lock bolts with a 1.00-in. (25-mm) pitch. Aluminum alloy bolts were used with the aluminum alloy stringers and steel bolts with the steel stringers. The sheet and stringer materials were match drilled for an interference fit with the bolts. Bolts were not installed along the transverse center line of the panels. The panels were made with the rolling direction of the sheet and stringer materials parallel to the longitudinal axis of the panels. A crack starter notch 0.50 in. (12.7 mm) long by 0.01 in. (0.24 mm) wide was made in the sheet material at the center

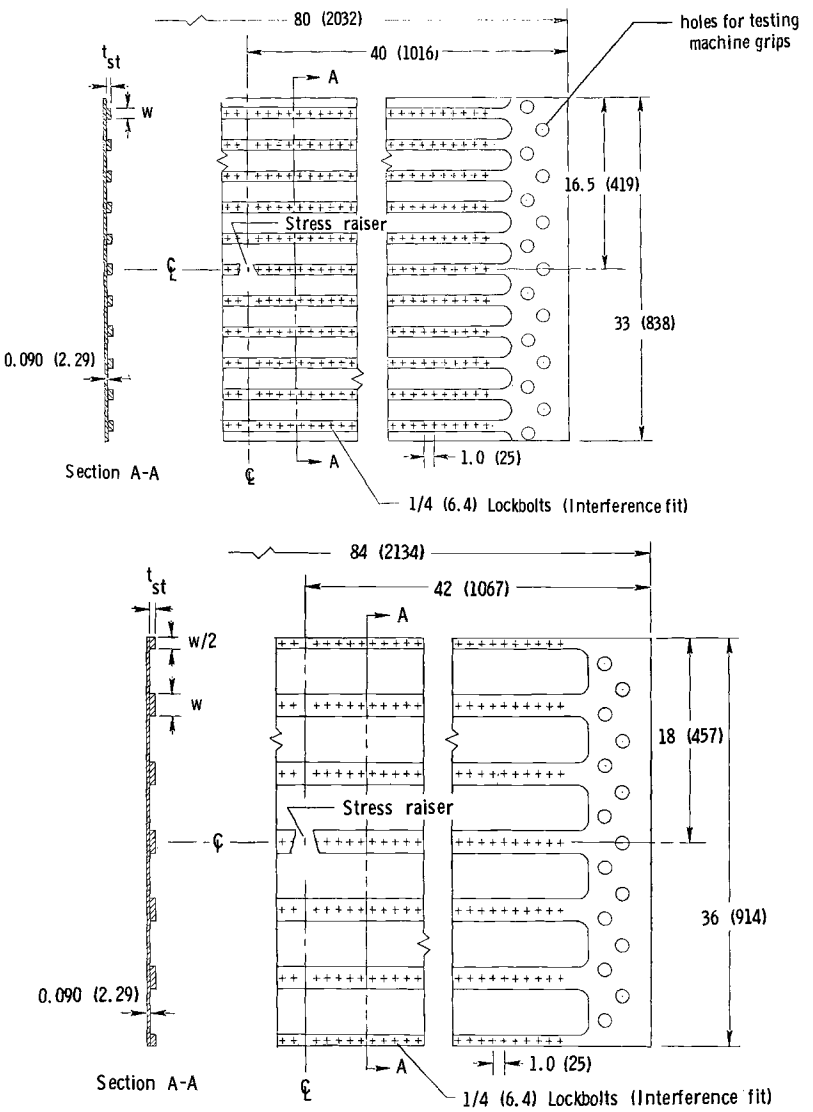

FIG. 1—*Panels with bolted stringers: top, 3-in. (76-mm) stringer spacing; bottom, 6-in. (152-mm) stringer spacing. Dimensions are in inches (millimeters).*

of each panel by an electrical discharge machining process. The tensile properties of the sheet and stringer materials were determined from standard ASTM tension specimens and are given in Table 2.

Panels with Integral Stringers

Three panels were fabricated from 7075-T6 sheets that had been extruded with integral stringers. The configuration of these panels is shown in Fig. 2.

TABLE 1—*Stiffened panels with bolted stringers.*

Stringer Material	Stringer Stiffness, μ	Stringer Spacing, b, in. (mm)	Stringer Thickness, t_{st}, in. (mm)	Stringer Width, w, in. (mm)
2024–T3.....	0.21	6.0 (152)	0.071 (1.80)	2.0 (51)
2024–T4.....	0.58	6.0 (152)	0.375 (9.53)	2.0 (51)
2024–T3.....	0.41	6.0 (152)	0.190 (4.83)	2.0 (51)
2024–T3.....	0.41	3.0 (76)	0.190 (4.83)	1.0 (25)
AM350–CRT.....	0.41	6.0 (152)	0.050 (1.27)	2.5 (64)
AM350–CRT.....	0.41	3.0 (76)	0.050 (1.27)	1.3 (32)

The stiffness ratio μ for these panels is 0.22. A crack starter notch 0.10 in. (2.54 mm) long by 0.01 in. (0.25 mm) wide was made in the center of each panel by an electrical discharge machining process. Rectangular aluminum blocks were adhesively bonded to the extruded panels at the ends to provide a firm and even surface for the testing machine grips. The tensile properties of these extrusions are given in Table 2.

Unstiffened Panels

Twelve unstiffened panels, 12 in. (300 mm) wide by 35 in. (890 mm) long, were made from the 0.090-in. (2.29-mm)-thick 2024-T3 aluminum alloy sheet. Two of these specimens were made from the remnant of each piece of material that had been used in making the sheet portion of the stiffened panels in Table 1.

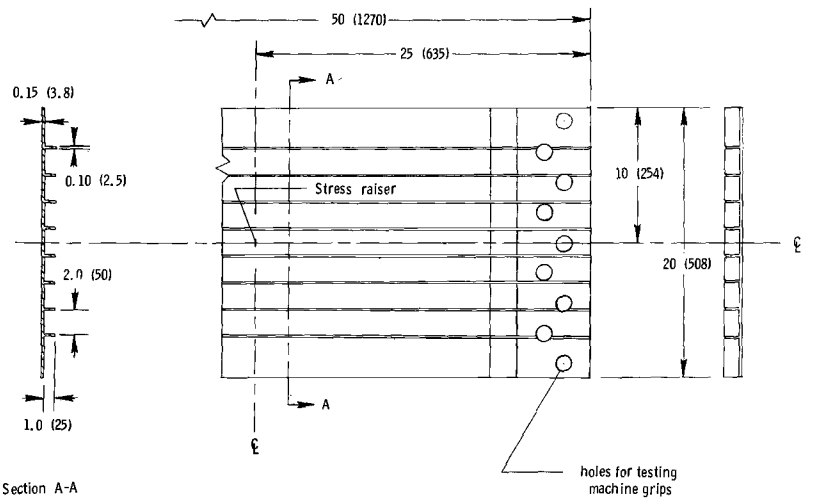

FIG. 2—*Panels with integral stringers. Dimensions are in inches (millimeters).*

TABLE 2—*Average tensile properties of sheet and stringer materials (longitudinal grain direction).*

Material	Thickness in. (mm)	Ultimate Tensile Strength, ksi (MN/m^2)	Yield Stress (0.2 percent Offset), ksi(MN/m^2)	Young's Modulus of Elasticity, ksi (GN/m^2)	Elongation in 2-in. (51-mm) Gage Length, Percent	No. of Tests
2024-T3	0.071 (1.80)	72.7 (501)	54.1 (373)	10 400 (71.7)	18	10
2024-T3	0.090 (2.29)	71.4 (492)	52.9 (365)	10 400 (71.7)	19	21
2024-T3	0.190 (4.83)	69.7 (481)	55.0 (379)	10 600 (73.1)	18	10
2024-T4	0.375 (9.53)	71.5 (493)	60.4 (416)	10 700 (73.8)	17	6
7075-T6[a]	0.156 (3.96)	85.9 (592)	78.1 (538)	10 300 (71.0)	11.5	...
AM350-CRT	0.050 (1.27)	230 (1590)	217 (1500)	28 400 (196)	22	6

[a] Extruded material—data taken from Ref *3*.

Three unstiffened panels, 20 in. (508 mm) wide by 50 in. (1270 mm) long, also were made from the 7075-T6 extruded sheets. One of these specimens was made from the remnant of each piece of material that had been used in making the integrally stiffened panels in Fig. 2. The stringers were machined from the extruded sheets.

A crack starter notch 0.10 in. (2.54 mm) long by 0.01 in. (0.25 mm) wide was made in the center of all the unstiffened panels. An electrical discharge machining process was used to make the notches.

Test Equipment and Procedure

All of the panels were subjected to axial cyclic loading of constant amplitude. The numbers of cycles required for the fatigue crack to reach various lengths were recorded. Loading was discontinued when the crack had extended across one third to one half the width of the specimen. Readings were made typically at 0.05-in. (1.3-mm) increments of crack length using 10-power microscopes mounted on an adjustable slide assembly with a scale and vernier. The scale and vernier could be read to within 0.001 in. (0.025 mm).

All of the specimens with the exception of the 2024-T3 unstiffened panels were tested in a 400,000-lbf (1780-kN) axial load, fatigue testing machine. Loading is controlled in this machine by a servohydraulic system capable of a wide range of loading frequencies. The 2024-T3 unstiffened panels were tested in a 132,000-lbf (590-kN) axial load, fatigue testing machine. This machine operates subresonantly at 820 cpm (14 Hz) or hydraulically at 40 cpm (0.7 Hz). Loading frequencies for all the tests were in the range 30 to 820 cpm (0.5 to 14 Hz). The lower frequencies were necessary to provide time for the crack length measurements when the crack growth rates were high.

The gross stresses in the sheet and stringers, respectively, were calculated in terms of the applied load P as follows:

$$S = \frac{P}{A + A_{st}E_{st}/E} \quad \ldots\ldots\ldots\ldots\ldots\ldots\ldots\ldots (2)$$

and

$$S_{st} = SE_{st}/E \quad \ldots\ldots\ldots\ldots\ldots\ldots\ldots\ldots (3)$$

Equations 2 and 3 were derived by assuming the sheet and stringers were equally strained by the applied load P. For the 2024-T3 aluminum alloy sheet material, the maximum cyclic value of gross stress in the sheet was 15.0 ksi (103 MN/m^2). For the panels with steel stringers, the stress in the stringers was nearly three times the stress in the aluminum alloy sheet. The maximum cyclic stress for the stiffened and unstiffened panels made with 7075-T6 aluminum alloy extrusions was 10.0 ksi (68.9 MN/m^2). The load ratio R was 0.10 for all tests.

In the tests of the stiffened panels with bolted stringers, one crack tip advanced more rapidly than the other. When the difference in crack length

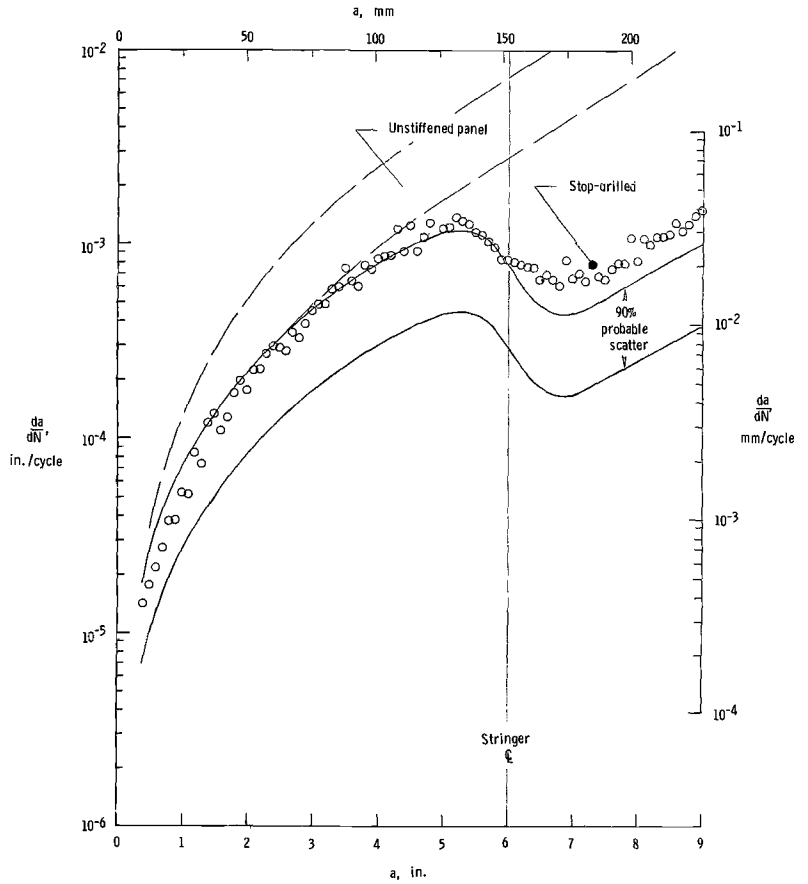

FIG. 3—*Predicted and measured rate of crack growth in panels with bolted stringers.* (a) $\mu = 0.21$, *aluminum alloy stringers spaced at 6 in. (152 mm).*

relative to the center line of the panel became more than 0.5 to 2.0 in. (13 to 51 mm), symmetry was restored by one of the following procedures: the laggard crack tip was extended with a jeweler's saw to the same distance from the panel center line as the other crack tip, or the advance crack tip was stop drilled to allow the laggard crack tip to catch up to the advance crack tip.

Axial load, residual static strength tests were conducted on the unstiffened panels following the fatigue crack growth tests. The specimens were loaded to failure at a stress rate of 30 ksi/min (3.4 MN/m²/s) and 100 ksi/min (11.5 MN/m²/s) for the 2024-T3 and 7075-T6 panels, respectively.

The 2024-T3 unstiffened panels were restrained from buckling in the vicinity of the crack by means of two heavy plates, one located on each side of the specimen. The plates were clamped together with a small clearance between

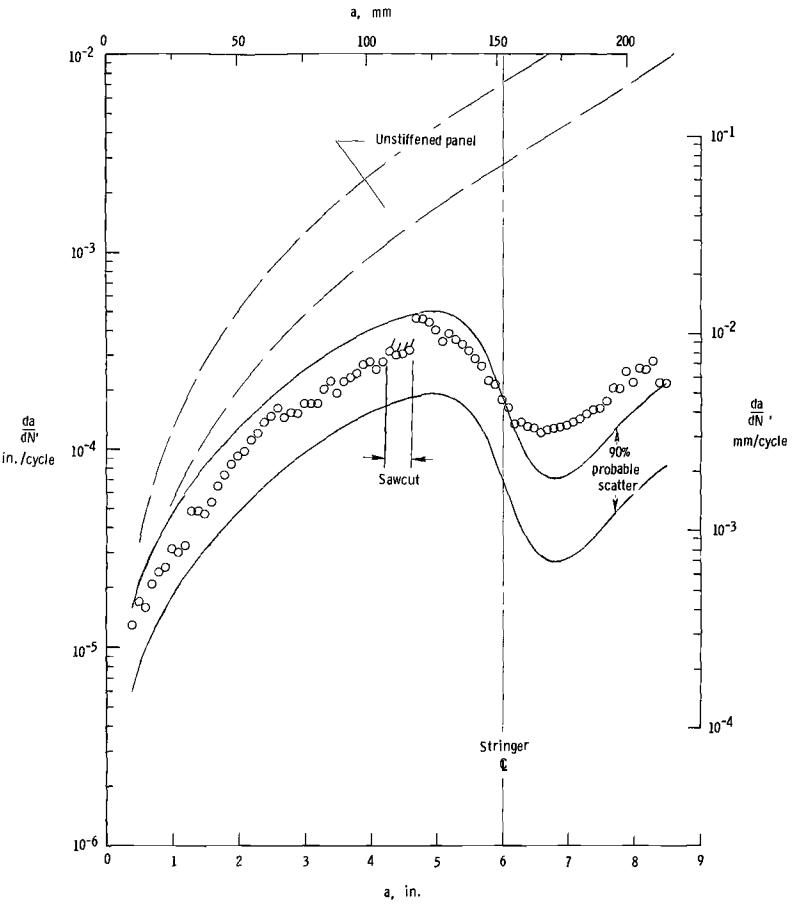

FIG. 3—*Continued.* (b) $\mu = 0.58$, *aluminum alloy stringers spaced at 6 in. (152 mm).*

the plates and the specimen. A slot 1.5 in. (38 mm) wide was made across the width of one plate so that the crack could be observed.

Results and Discussion

The K-rate relationships for the 2024-T3 and 7075-T6 unstiffened panels are given in Appendix I. An analysis of the scatter in the K-rate relationships also is given. The stress intensity factor-crack length relationships for the panels with bolted and integral stringers are given in Appendix II.

Figures 3 and 4 show the measured and predicted crack growth rates plotted against half crack length for the stiffened panels with bolted stringers and with integral stringers, respectively. The measured rates were determined by numerically differentiating the relationship between crack length and load cycles. The derivatives were calculated for each crack length measurement

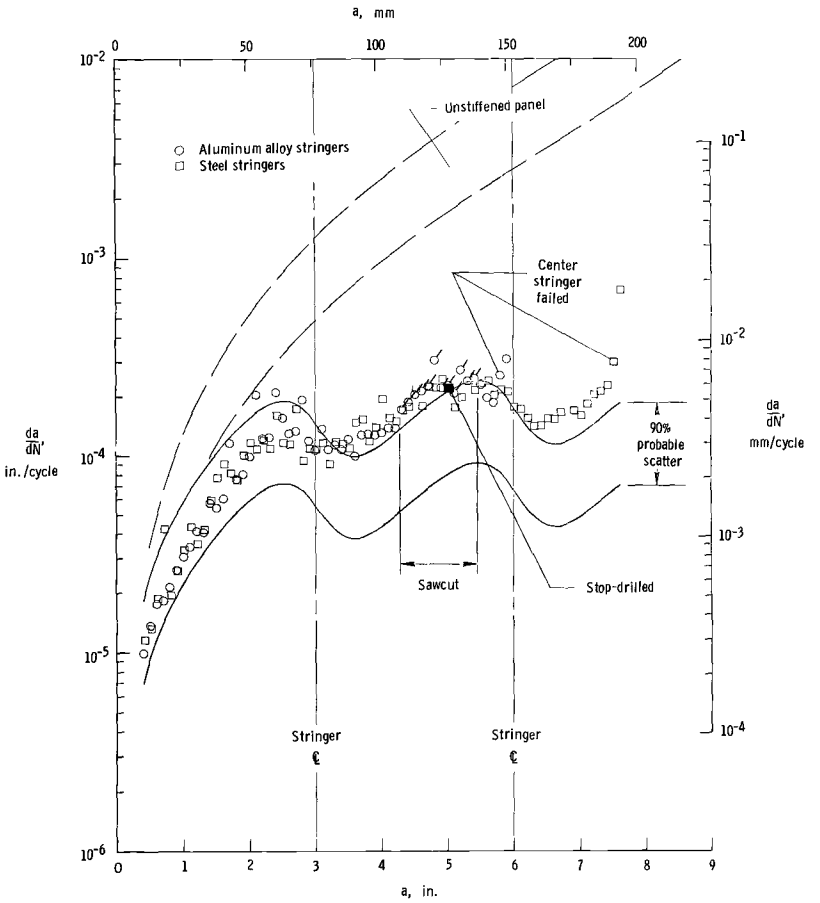

FIG. 3—*Continued.* (c) $\mu = 0.41$, *aluminum alloy and steel stringers spaced at 3 in. (76 mm).*

using Lagrange's interpolation formula of second degree [*4*]. The plotted values represent the average for both crack tips except where a crack tip was extended with a jeweler's saw or was stop drilled. In those cases the rate for the unaltered crack tip, shown as a ticked or filled symbol, respectively, was plotted in lieu of an average value. The general continuity of the rates measured before and after a saw cut was made indicates that the absence of symmetry had little effect upon the stress intensity factor. The predicted rates are shown in each figure as a band representing a probable scatter. The curves defining this band represent the fifth and ninety-fifth percentiles of the scatter in the K-rate relationship; thus, 90 percent of the rates should be within the band. The predicted rates for an unstiffened panel with the same applied stress also are shown in each figure for comparison. The stress intensity factor for an unstiffened sheet, $K = S\sqrt{\pi a}$, was used in making these calculations.

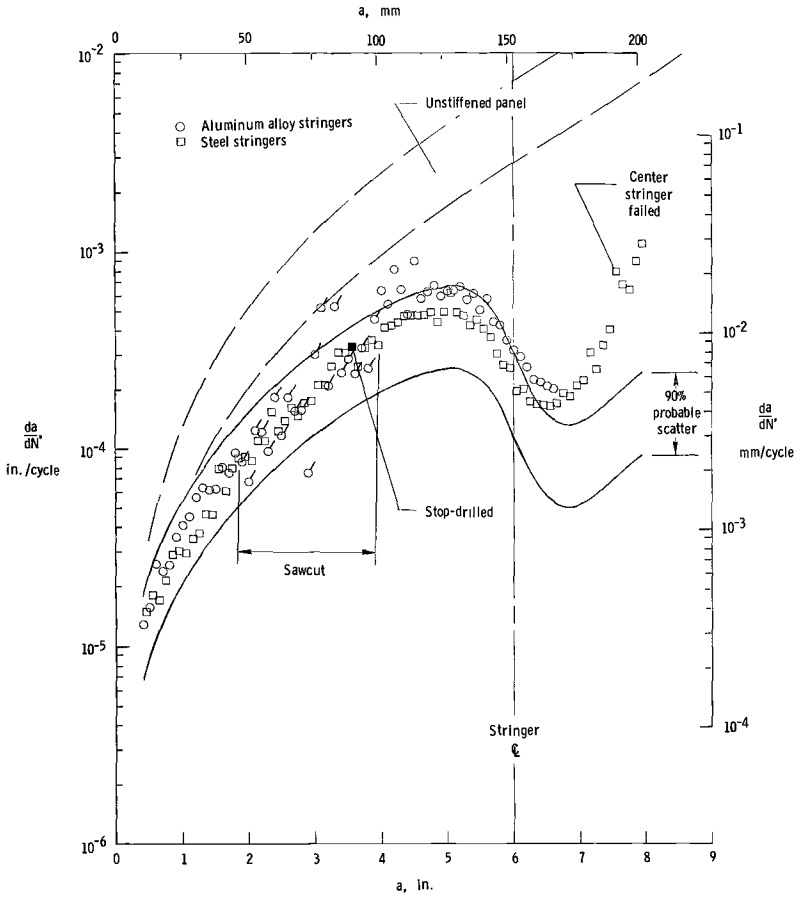

FIG. 3—*Continued.* (d) $\mu = 0.41$, *aluminum alloy and steel stringers spaced at 6 in. (152 mm).*

Panels with Bolted Stringers

The measured and predicted crack growth rates in Fig. 3 show that the method correctly predicted the rates for the panels with bolted stringers, except that the measured rates were slightly higher than the predicted rates when the crack tip was beyond the first stringer. Two major factors contribute to these differences. First, the forces on the bolts nearest the crack became very high when the crack advanced beneath a stringer, and the bearing stresses around the holes exceeded the bearing yield strength of the sheet material. Thus, the stringers were not as effective in reducing the crack tip stresses as had been indicated by the calculated value of the stress intensity factor. Second, because the sheet and stringers were not coplanar, the crack in the sheet caused bending stresses to develop in the center of the panel. These bending stresses, which increase with crack length, were not considered in the stress intensity factor calculations. Strain gage measurements revealed

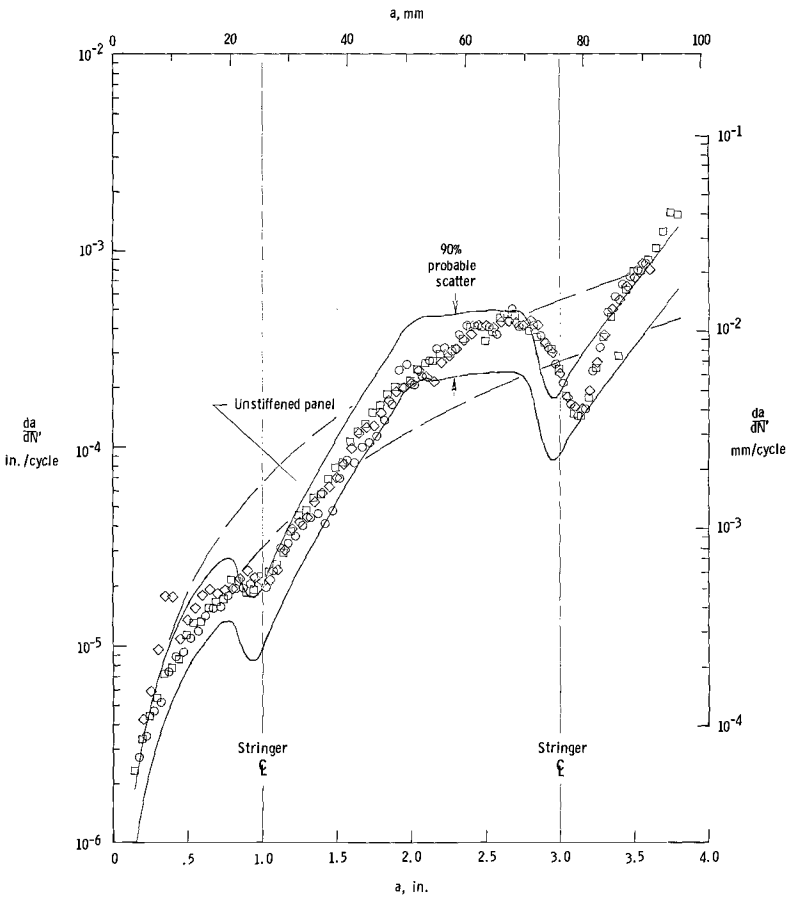

FIG. 4—*Predicted and measured rate of crack growth in panels with integral stringers. Symbols denote three tests.*

that the bending stresses near the crack tips could be as large as one fourth of the axial stresses when the crack was long.

The results in Fig. 3 also show that the stress intensity factor correctly predicted the lower crack growth rates for the panels with stiffer and more closely spaced stringers. Furthermore, the results show that the stress intensity factor correctly predicted equal rates for the equivalent panels with steel and with aluminum alloy stringers. The predicted rates for the panels with bolted stringers, especially those with stiffer and more closely spaced stringers, generally are much lower than the rates for equally stressed unstiffened panels. Thus, the bolted stringers were effective in reducing crack growth rates.

The center stringer failed in both of the panels with stringers spaced at 3 in. (76 mm) and in the panel with steel stringers spaced at 6 in. (152 mm)

(see Figs. 3*c* and 3*d*). Fatigue crack growth rates were noticeably higher immediately thereafter indicating the detrimental effect of a broken stringer. The fatigue cracks that caused the failures always initiated in one of the two bolt holes nearest the crack in the center stringer. The calculated stress in the stringer at the center of the panel is higher for the panels with the smaller stringer spacing [*2*]; thus, fatigue failures should be more likely to occur in the stringers of the panels with 3-in. (76-mm) strap spacing.

Panels with Integral Stringers

The measured and predicted crack growth rates in Fig. 4 show that the method also correctly predicted the rates for the panels with integral stringers except when the crack tip is in the immediate vicinity of a stringer. In these cases, the measured rates are higher than the predicted rates, indicating that the calculated stress intensity factor is too low. The predicted curves for an unstiffened panel are not significantly different from the curves for an equally stressed panel with integral stringers. The integral stringers did not cause any overall reduction in the crack growth rates.

The solid symbols in Fig. 5 show the measured crack growth rates in the stringers of one of the integrally stiffened panels. For comparison, the rate of growth of the crack in the sheet also is shown and is plotted in open symbols. For convenience, both crack lengths were made nondimensional by

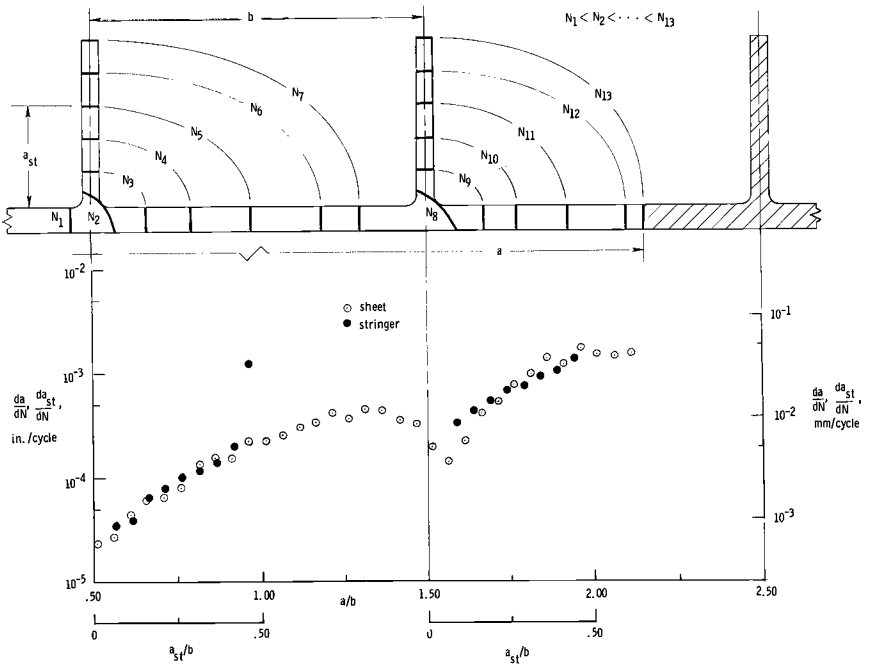

FIG. 5—*Measured rate of crack growth in stringers of integrally stiffened panel.*

dividing by the stringer spacing. The results show that the rates are essentially the same for both crack tips. The lines in the sketch at the top of the figure show the crack front at various cycles of load. The crack tips developed straight fronts normal to the direction of growth shortly after the crack branched at each stringer. Also, the stringers failed when the crack tip in the sheet was approximately 1.5 in. (38 mm) beyond the stringer. This distance is larger than that assumed in estimating the stress intensity factor; however, this discrepancy caused only slight disagreement between the measured and predicted rates.

Summary

The rate of growth of a fatigue crack was measured in fatigue tests of stiffened panels with bolted stringers and with integral stringers. Stringer spacing, stringer stiffness, and stringer material were varied systematically in the panels with bolted stringers. A probable scatterband of crack growth rates was predicted for the stiffened panels on the basis of a K-rate relationship determined from tests of unstiffened sheets and of stress intensity factor calculations for the stiffened panels.

The stress intensity factor calculated by the method in Ref *2* correctly predicted the crack growth rates in the panels with bolted stringers except when the crack was long. In these cases the measured rates were slightly higher than the predicted rates. The calculated stress intensity factor correctly predicted the crack growth rates to be lower in the panels with stiffer and more closely spaced stringers and to be the same in panels with steel and with aluminum alloy stringers of equal stiffness. For longer cracks, the bolted stringers caused a significant reduction in crack growth rates compared to an equally stressed unstiffened panel.

The stress intensity factor calculated for the stiffened panels with integral stringers also correctly predicted the crack growth rates. The stress intensity factor was estimated satisfactorily by assuming the integral stringers to be attached to the sheet with closely spaced rivets and by assuming the crack to branch at each stringer and grow simultaneously through the sheet and stringer at the same rate. Also, as predicted, the integral stringers had an insignificant effect on the crack growth rates compared with an equally stressed unstiffened panel.

APPENDIX I

Relationship Between Stress Intensity Factor and Crack Growth Rate

In Fig. 6 the values of crack growth rate measured in the tests of the unstiffened panels are plotted against the range of the stress intensity factor, ΔK. The values of ΔK were calculated by the following equation:

$$\Delta K = S_{\max} (1 - R)\sqrt{W \tan (\pi a/W)} \quad \ldots\ldots\ldots\ldots\ldots\ldots (4)$$

where $S_{\max}$ is the maximum cyclic stress and W is the width of the unstiffened panel.

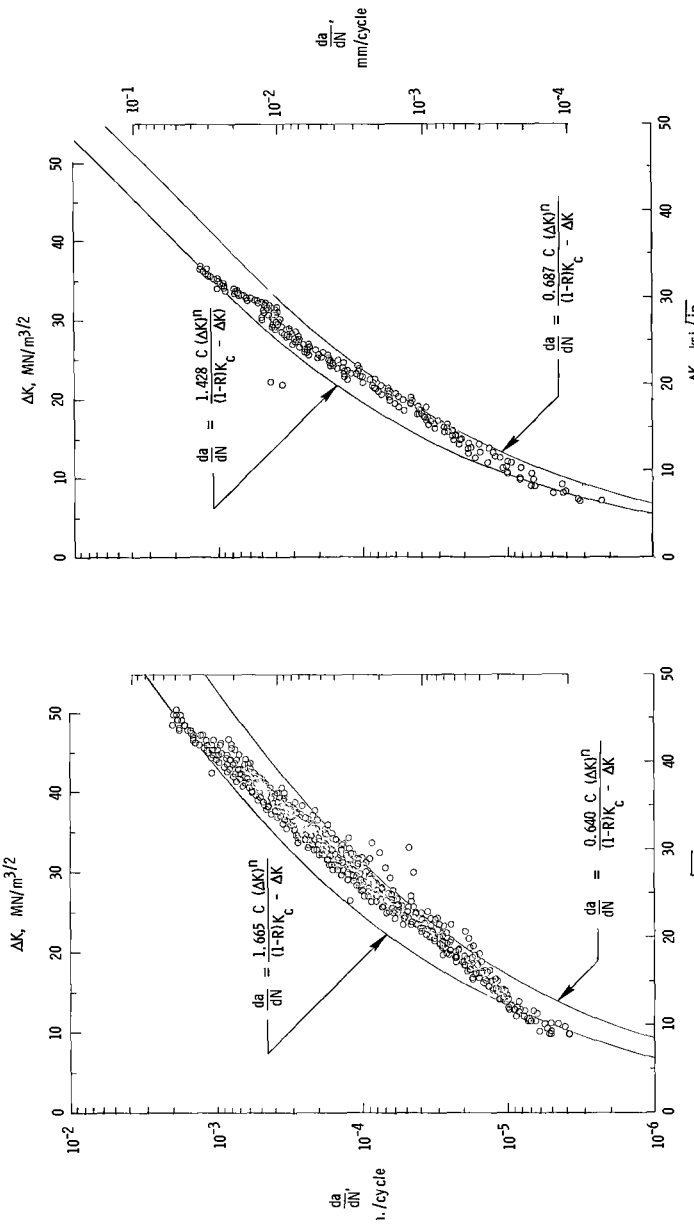

FIG. 6—K-*rate measurements in unstiffened panels of (left) 2024-T3 and (right) 7075-T6 aluminum alloy.*

The rate of crack growth with respect to cycles of load was calculated by numerically differentiating the crack length-cycles measurements. The differentiation was carried out using Lagrange's interpolation formula of second degree [*4*].

For convenience, an empirical equation proposed by Forman [*5*] was used to represent the K-rate relationship mathematically. Hudson [*6*] has shown that this equation provides an excellent mathematical representation of the K-rate relationship for both 2024-T3 and 7075-T6 aluminum alloys with various values of mean and alternating load. This equation gives the rate of crack growth with respect to cycles of load as

$$\frac{da}{dN} = \frac{C(\Delta K)^n}{(1 - R)\,K_c - \Delta K} \quad \ldots\ldots\ldots\ldots\ldots\ldots\ldots\ldots (5)$$

where K_c is the critical value of the stress intensity factor and C and n are constants.

The values of K_c used in Eq 5 were determined from the residual static strength tests of the panels without stiffeners. The values of the constants C and n were determined by a least squares fit of Eq 5 to the K-rate measurements. The values of K_c, C, and n for the two alloys are given in the following table:

Material	K_c, ksi $\sqrt{\text{in.}}$	K_c, MN/m$^{3/2}$	C[a]	n[a]
2024–T3	92	101	2.165×10^{-15}	3.50
7075–T6	68	75	1.046×10^{-14}	3.40

[a] These values are for U.S. customary units only.

The error that was minimized in the least squares fit of Eq 5 to the K-rate measurements in Fig. 6 is defined by

$$\ln \epsilon = \ln (da/dN)_m - \ln (da/dN) \quad \ldots\ldots\ldots\ldots\ldots\ldots\ldots (6)$$

where $(da/dN)_m$ is the measured crack growth rate, da/dN is the crack growth rate calculated by Eq 5, and $\ln \epsilon$ is the error. Substituting Eq 5 into Eq 6, ϵ can be written as

$$\epsilon = \frac{(da/dN)_m}{\dfrac{C(\Delta K)^n}{(1 - R)\,K_c - \Delta K}} \quad \ldots\ldots\ldots\ldots\ldots\ldots\ldots\ldots (7)$$

The cumulative distribution of ϵ for the measurements in Fig. 6 is shown in Fig. 7. The values of ϵ that represent the fifth and ninety-fifth percentiles of ϵ are given in the following table:

Material	ϵ, $F(\epsilon) = 0.05$	ϵ, $F(\epsilon) = 0.95$
2024–T3	0.640	1.665
7075–T6	0.687	1.428

The fifth and ninety-fifth percentiles of the measured rates were obtained by multiplying Eq 5 by the corresponding values of ϵ in the table. The resulting equations are shown in Fig. 6 with the measured rates.

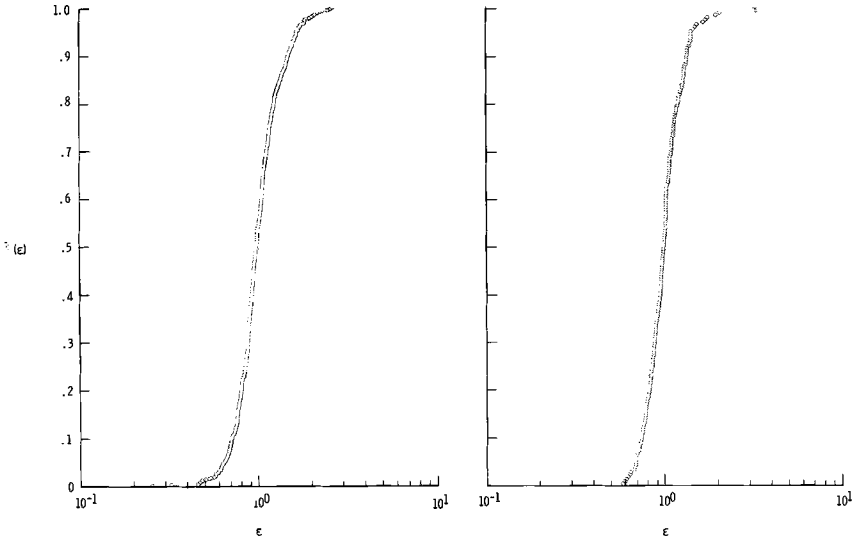

FIG. 7—*Cumulative distribution of* ϵ *for* K*-rate measurements in tests of unstiffened panels of (left) 2024-T3 and (right) 7075-T6 aluminum alloy.*

APPENDIX II

Stress Intensity Factor Calculations for Stiffened Panels

The stress intensity factor for the stiffened panels was calculated by a previously developed method [*2*] that accounted for riveted stringers of uniform size and spacing. Figure 8 shows the stress intensity factor for each panel with bolted stringers in Table 1 plotted against half crack length. The curves for $\mu = 0.41$ represent a panel with aluminum alloy stringers and a panel with steel stringers. For convenience, the stress intensity factor and the half crack length are made nondimensional by dividing by the stress intensity factor of an unstiffened sheet, $S\sqrt{\pi a}$, and the stringer spacing, b, respectively.

The stress intensity factor for the panels with integral stringers was calculated by assuming that the stringers were attached to the sheet with very closely spaced rivets. As the rivet spacing approaches zero, this situation approaches the case of integral stringers. Figure 9*a* shows the stress intensity factor plotted against half crack length for a value of rivet spacing of $p/b = 1/15$. Preliminary calculations revealed that smaller values of rivet spacing would not alter the results. The stress intensity factor and the half crack length are made nondimensional by dividing by $S\sqrt{\pi a}$ and b, respectively. Because a fatigue crack advances through an integral stringer as well as through the sheet itself, the calculations were made with the assumption that the stringers intersecting the crack were severed completely by the crack. The large discontinuities in the curve are a result of load transfer from the severed stringers to the sheet in the immediate vicinity of the crack tip. These discontinuities are unrealistic because the stringers are not likely to be severed completely until the crack tip in the sheet has advanced some distance beyond the stringers. The curve was modified in Fig. 9*b* to approximate the behavior of the stringer as the crack branches and proceeds simultaneously through the sheet and stringer. The crack

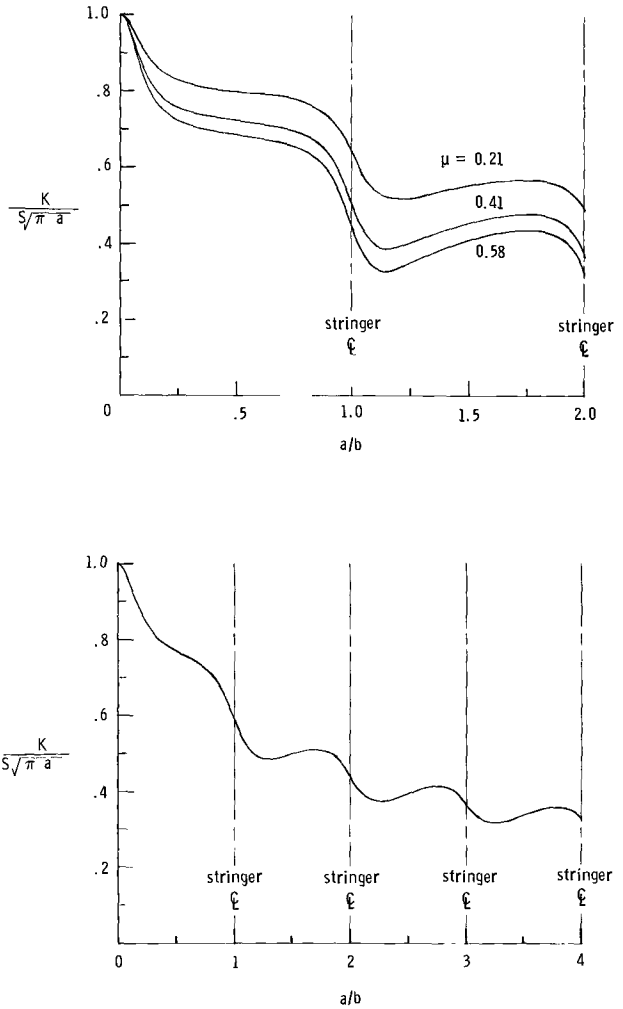

FIG. 8—*Relationship between stress intensity factor and crack length for panels with bolted stringers: top, 6-in. (152-mm) stringer spacing; bottom, 3-in. (76-mm) stringer spacing;* $\mu = 0.41$.

growth rate was assumed to be equal in the sheet and stringer so that the stringer is not severed completely until the crack in the sheet has advanced an additional distance equal to the height of the stringer. Between the edge of the stringer and the point at which the stringer is assumed to be severed completely, $K/S\sqrt{\pi a}$ was assumed to increase linearly with a/b, as shown.

References

[*1*] Figge, I. E. and Newman, J. C., Jr., "Prediction of Fatigue-Crack-Propagation Behavior in Panels with Simulated Rivet Forces," NASA TN D-4702, National Aeronautics and Space Administration, 1968.

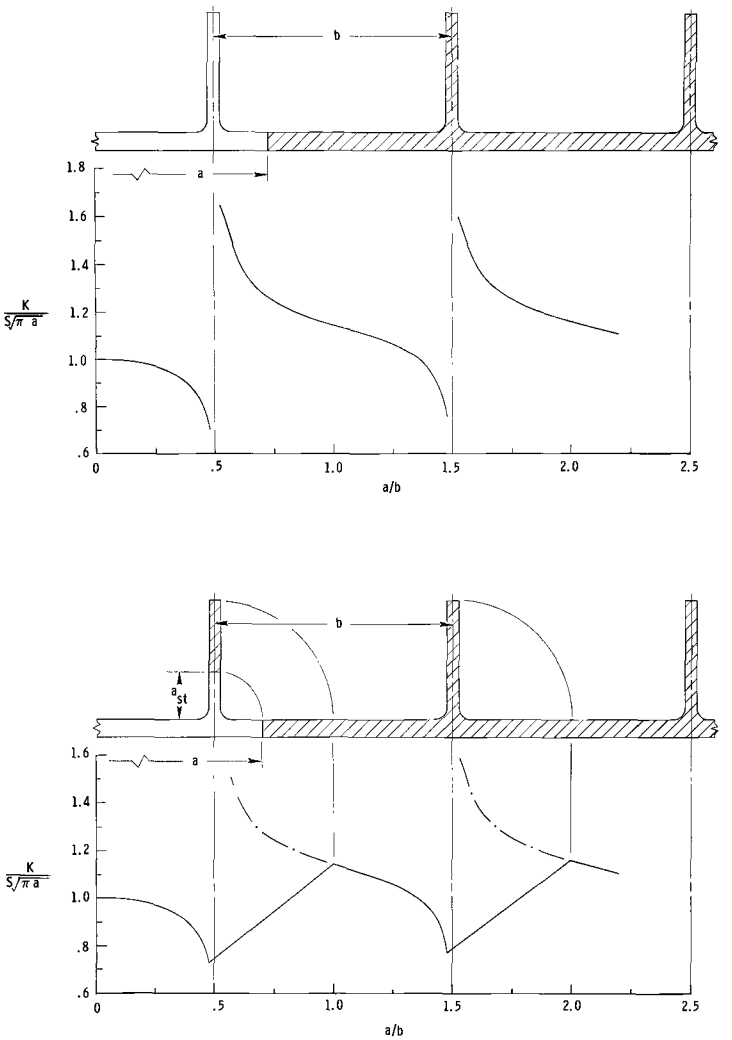

FIG. 9—*Relationship between stress intensity factor and crack length for panels with integral stringers: top, completely severed stringers; bottom, partially severed stringers.*

[2] Poe, C. C., Jr., "The Effect of Riveted and Uniformly Spaced Stringers on the Stress Intensity Factor of a Cracked Sheet," M.S. thesis, Virginia Polytechnic Institute, 1969.

[3] Leybold, H. A., "Residual Static Strength of Aluminum-Alloy Box Beams Containing Fatigue Cracks in the Tension Covers," NASA TN D-796, National Aeronautics and Space Administration, 1961.

[4] Neilson, K. L., *Methods in Numerical Analysis*, second ed., Macmillan Co., 1965, pp. 150–154.

[5] Forman, R. G., Kearny, V. E., and Engle, R. M., *Journal of Basic Engineering, ASME Transactions*, Series D, JBAEA, Vol. 89, No. 3, Sept. 1967, pp. 459–464.

[6] Hudson, C. M., "Effect of Stress Ratio on Fatigue-Crack Growth in 7075-T6 and 2024-T3 Aluminum Alloy Specimens," NASA TN D-5390, National Aeronautics and Space Administration, 1969.